

# Arc Instabilities in a Plasma Spray Torch

Z. Duan and J. Heberlein

(Submitted 16 October 2000)

The control over coating quality in plasma spraying is partly dependent on the arc and jet instabilities of the plasma torch. Different forms of instabilities have been observed with different effects on the coating quality. We report on an investigation of these instabilities based on high-speed end-on observation of the arc. The framing rate of 40,500 frames per second has allowed the visualization of the anode attachment movement and the determination of the thickness of the cold-gas boundary layer surrounding the arc. The images have been synchronized with voltage traces. Data have been obtained for a range of arc currents, and mass flow rates for different gas injectors and for anodes displaying different amounts of wear. The analysis of the data has led to quantitative correlations between the cold-gas boundary layer thickness and the instability mode for the range of operating parameters. The arc instabilities can be seen to enhance the plasma jet instabilities and the cold-gas entrainment. These results are particularly useful for guiding plasma torch design and operation in minimizing the influence of plasma jet instabilities on coating properties.

**Keywords** control, diagnostics, plasma spraying, torch instabilities

## 1. Introduction

It has been well known that the coating quality of plasma spraying is strongly influenced by plasma instability.<sup>[1-4]</sup> In a direct-current plasma torch similar to those used in spraying, the arc gas is introduced from the base of the cathode. The cathode usually has a cone shape, and the arc cathode attachment is stable at the tip of the cathode. However, the arc anode attachment is perpendicular to the gas flow and nozzle axis and is exposed to a strong, dynamic drag force resulting from the interaction between the gas flow and the arc anode attachment. This interaction will keep the anode attachment continuously fluctuating. This fluctuation of the arc attachment has a period that is similar in magnitude to the transition time of the spray particle in the plasma jet (0.1 to 1 ms). Furthermore, the arc instability can affect the overall performance of a torch, such as average arc voltage and torch efficiency. In addition to the jet turbulence and the powder injection characteristics, the arc instability plays one of the important roles in determining particle heating and final coating quality. The arc instability exists not only in the plasma spray torch but also in many other arcing devices.

To investigate the arc dynamical characteristics requires diagnostic techniques with high time resolution. The voltage waveform is the most convenient and direct method to analyze the arc instability. However, in many cases, it is very difficult to interpret the voltage waveform since there are several factors affecting the arc voltage. The voltage waveforms can give more information if coupled with high-speed photography.

In this paper, we will present experimental results on arc dynamics investigation using voltage waveform analysis and high-speed photography. The arc dynamic behavior has been ob-

served for various operating parameters and anodes that have different levels of wear. The research has concentrated on determining the thickness of the cold-gas boundary layer between the arc column and the anode surface and the correlation between the boundary layer thickness and the arc characteristics.

## 2. Experimental Setup and Procedures

The investigation has been carried out with a Praxair SG-100 plasma-spray torch operating in the subsonic mode. A #2083-129 cathode and a #2083-720 anode have been used. The anode has a straight bore nozzle with an 8 mm diameter and 25 mm in length. In order to examine the effects of anode deterioration, three #2083-720 anodes with different levels of wear have been used. One of these anodes, called the "new" anode, has less than 10 h service time. The second one, called the "used" anode, has about 50 h service time and less than 100 starts. The third one is a burnt-out anode that is called the "burnt" or the "strongly eroded" anode. These three anodes represent varying degrees of surface erosion. The depths of the erosion spots in these three anodes are less than 0.2 mm, about 0.8 mm, and about 1.5 mm, respectively. Three different gas-injector rings have been used. The #2083-113 has four tangential holes to introduce a swirling gas flow. The #2083-112 uses four radial holes to provide a straight gas flow. A customized gas injector, called 20% injector, combines four radial holes and two tangential holes providing a flow with 20% vortex and 80% straight flow.

The torch is operated with argon as the primary gas and helium as the secondary gas. The operating parameters include arc current, mass flow rate of the plasma gases, gas injection method, and anode condition. The ranges of these parameters are listed in Table 1.

In our experiments, arc voltages are directly sampled by a computer-controlled digital oscilloscope. In order to see enough details of the waveform and enough wave trains, the sampling rate is set to 100 kHz with 4096 points. The arc voltage is obtained as the difference of the cathode and anode potentials. In this way, the effect of the cable resistance is eliminated.

Z. Duan, Hypertherm, Inc., Hanover, NH 03755; and J. Heberlein, Department of Mechanical Engineering, University of Minnesota, Minneapolis, MN 55455. Contact e-mail: jvrh@me.umn.edu.

**Table 1 Plasma Torch Operating Conditions**

Parameters	Settings
Arc current	200 to 900 A
Primary gas	Argon: 40 to 120 slm
Secondary gas	Helium: 0 to 40 slm
Gas flow	Vortex, 20% vortex + 80% straight, straight
Anode diameter	8 mm, 10 mm
Anode condition	New, used, burnt

We have used the Kodak EKTAPRO HS Motion Analyzer, Model 4540 (Eastman Kodak Company, Rochester, NY), to capture sequences of the arc movement and the jet. The Kodak HS system is a high-speed video recording system with the ability to record up to 40,500 pictures (partial frames) per second. A frame consists of  $256 \times 256$  pixels with 256 gray levels, and at the highest framing rate, the picture is a segmented frame with  $28 \times 28$  pixels. The speed is higher than the usual plasma fluctuations, thus, allowing analysis and image storage of the plasma dynamic behavior. The digital memory installed in the processor can store 1024 frames of full screen. The processor can output the captured signals in very high frequency (VHS) and super-VHS format for immediate playback on a monitor or for being recorded with a connected video cassette recorder (VCR). The system can output a series of vertical synchronizing pulses at the beginning of each captured picture. This function is convenient for the synchronization of the arc voltage traces with the captured images. The oscilloscope has been triggered by the first pulse every time we start the image acquisition.

The images captured by the Kodak HS video system are transferred to a computer with a frame-grabber for storage and processing. The first 1000 frames of each acquisition have been recorded by a VCR onto videotapes. An optical system has been set up to capture the arc motion inside the nozzle.

We consider that the arc voltage waveform with some clearly defined characteristics indicates a type of “arc operating mode.” With argon/helium mixture operating in the SG-100 plasma spray torch, we can define three basic dynamic modes of the arc operation, as shown in Fig. 1. The arc operating modes illustrated here are obtained with the new anode and straight plasma-gas flow. The typical restrike-mode behavior is characterized by a large mean voltage and large voltage fluctuations with a sawtooth shape profile. However, the restrike waveform shown in Fig. 1 is obtained with a current of 100 A and a flow rate of 120/40 slm of argon-helium mixture, which is actually outside the range used in real spray applications. With increasing current and decreasing gas flow rate, the mean arc voltage is reduced, and the waveform shows a characteristic of a more or less sinusoidal shape with relatively low amplitudes. Such an arc operating characteristic has been referred to as the “fluctuating mode with takeover” or just the “takeover” mode. The takeover waveform, shown in Fig. 1, is obtained with a current of 500 A and a plasma-gas flow rate of 40/20 slm of an argon-helium mixture. It should be noted that most plasma spray operations with argon-helium mixtures fall into the range in which the takeover operating mode dominates. With a very high current and a straight gas flow, the arc may suddenly jump to the “steady” mode, which is represented by a very low mean voltage and a nearly flat profile. The steady mode presented in Fig. 1 is achieved with a current of 900 A and a pure argon flow of 60

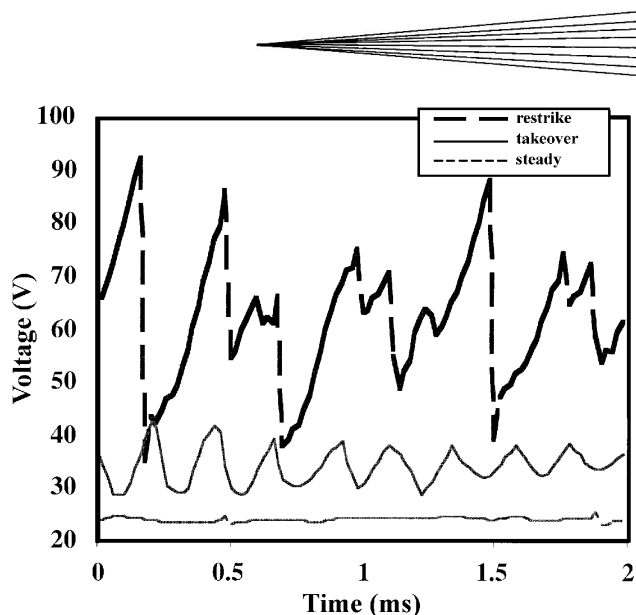


**Fig. 1** Basic arc operating modes. Restrike mode: 100 A, 12/40 slm of Ar/He; takeover mode: 500 A, 40/20 slm of Ar/He; and steady mode: 900 A, 60 slm Ar

slm. A very low torch efficiency is usually observed due to the low mean voltage.

The voltage waveforms, obtained over an extensive range of operating parameters, show the arc, in most cases, not in a perfectly distinct mode but with a mixed characteristic. The mixed characteristics could be either a combination of the restrike and the takeover modes or a combination of the takeover and the steady modes, as shown in Fig. 2. The mixed mode A, obtained with a current of 800 A and a pure argon gas flow of 100 slm, consists of the steady and the takeover modes. The mixed mode B, obtained with a current of 400 A and an argon/helium gas flow of 98/20 slm, consists of the restrike and the takeover modes.

In order to present and discuss results easily and clearly, the arc instability characteristic is assigned a numerical value in the following sections. This numerical value is referred to as the “mode value.” The restrike mode is equal to 2, the takeover mode equal to 1, and the steady mode equal to 0. While a perfect mode is assigned an integer, a decimal number between 0 to 2 specifies a mixed voltage fluctuating characteristic. For example, “mode = 1.2” represents a voltage mode consisting of an 80% takeover characteristic and a 20% restrike characteristic. To calculate the mode value, the shape of the voltage waveform is used to distinguish the restrike mode from the takeover mode, and the fluctuation amplitude is used to distinguish the takeover mode from the steady mode. A shape factor,  $S$ , and an amplitude factor,  $A$ , are calculated as follows:

$$S = \frac{t_{\text{up}}}{t_{\text{down}}} \quad (\text{Eq 1})$$

$$A = \frac{\Delta V}{V} \times 100\% \quad (\text{Eq 2})$$

where  $t_{\text{up}}$  is the time duration of the up-rising slope of the waveform,  $t_{\text{down}}$  is the time duration of the down slope of the wave-

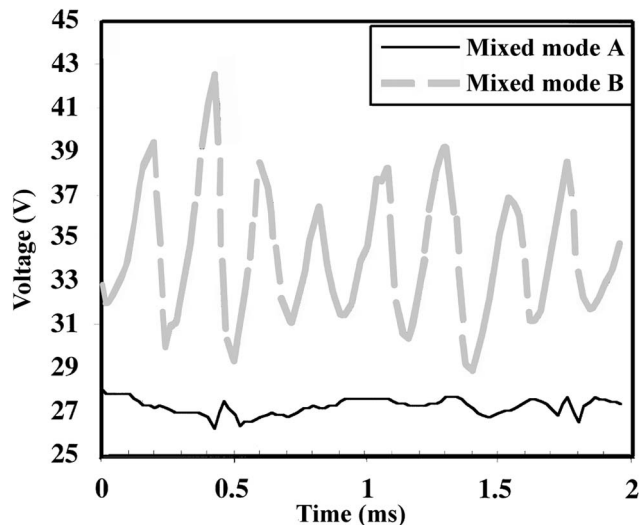


**Fig. 2** Mixed arc operating modes. Mixed mode A: 800 A, 100 slm Ar; and mixed mode B: 400 A, 98/20 slm Ar/He

form,  $\Delta V$  is the amplitude of the arc voltage fluctuation, and  $V$  is the mean arc voltage. We define:

If  $A \geq 10\%$  and  $S \geq 5$ , the arc mode is defined as running in perfect restrike mode, mode value = 2.

If  $A \geq 10\%$  and  $S < 1.1$ , the arc is defined as running in a perfect takeover mode, mode value = 1.

If  $A < 2\%$ , the arc is considered in a steady mode, mode value = 0.

If  $A \geq 10\%$  and  $S < 5$ , the arc is considered to be in a restrike-takeover mixing mode, mode value =  $1 + (S - 1.1)/3.9$ .

If  $2\% < A < 10\%$ , the arc is considered to be in a takeover-steady mixing mode, mode value =  $(A - 2\%)/8\%$ .

End-zone imaging is used to observe the cross section of the arc inside the nozzle and to estimate the thickness of the cold-gas boundary layer and the anode attachment location. Figure 3 shows a typical end-zone image and an intensity profile along the line, which crosses the arc column center. We define the edge of the cold-gas boundary layer as being located at the point where the intensity is half of the highest intensity inside the nozzle channel. Since the radiation energy has a rapid rise between 5000 and 8000 K for an argon-based plasma, the above definition will locate the boundary layer edge at a point where the temperature is about 6500 K. The thickness of the boundary layer, which is the distance from the edge to the nozzle wall, is then converted from a number of pixels to a physical dimension in mm. The accuracy of the boundary-layer thickness measurement is determined by how accurately the edge of the arc can be determined on the image captured by the computer. The maximum error is judged to be two pixels, which corresponds to 0.1 mm in boundary-layer thickness value. Since the arc is in a highly fluctuating state, the thickness of the boundary layer has been measured ten times for each individual experimental condition to obtain an average value and reduce the error. Among these ten measurements, the boundary layer thickness usually varies  $\pm 25\%$  from the average value. The statistical standard deviation over these ten measurements is about 0.15 mm. The po-

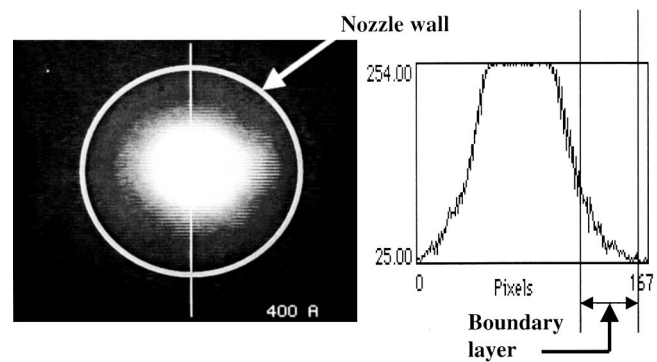


**Fig. 3** Boundary layer measurement in an end-on arc image, anode diameter 8 mm

sition of the anode attachment is also identified from the end-zone image if it is visible.

The definition of the boundary layer based on changes in radiation intensity is, in our opinion, justified for the following reasons. The radiation emitted from a plasma is strongly and uniquely related to the temperature,<sup>[5]</sup> showing a particular strong increase in the range between 5000 and 12,000 K. Because of this strong increase, the radiation intensity will have an even stronger radial gradient than the temperature does, and the dark region between the luminous arc core and the anode-nozzle wall can be considered a good representation for the thermal boundary layer. Furthermore, we believe that these boundary layer measurements also give a good approximation for the concentration boundary layer. In local thermodynamic equilibrium (LTE), the increase in electron concentration follows closely the increase in radiation emission. Although we have to expect some deviations from LTE because of electron diffusion effects in the arc fringes, the high pressure in the arcing region will limit these effects.

While changes of arc current, total mass flow rate, nozzle shape, and gas injector type does influence the boundary layer, they do not affect the measurement technique based on the preceding arguments. However, a change in the ratio of argon to helium gas will affect the emission not only by a change in temperature distribution but also by a change in the concentration of radiating species. Helium will contribute little to the emitted radiation because of its much higher excitation energies, but it will reduce the density of excited argon atoms. This dilution should be uniform over the cross section of the arc. Consequently, the radial distribution of the radiation intensity still reflects the radial distribution of the temperature, even though the absolute values will be different.

### 3. Results and Discussions

With end-on observation using the high-speed video camera, the first observation made is the continuous movement of the arc attachment in the restrike mode. It has previously been observed that the arc has two types of restrike modes.<sup>[4,6,7]</sup> The first one is a downstream movement of the arc attachment with the gas flow and a subsequent upstream breakdown. The other mode is characterized by a distortion of the arc attachment channel while the

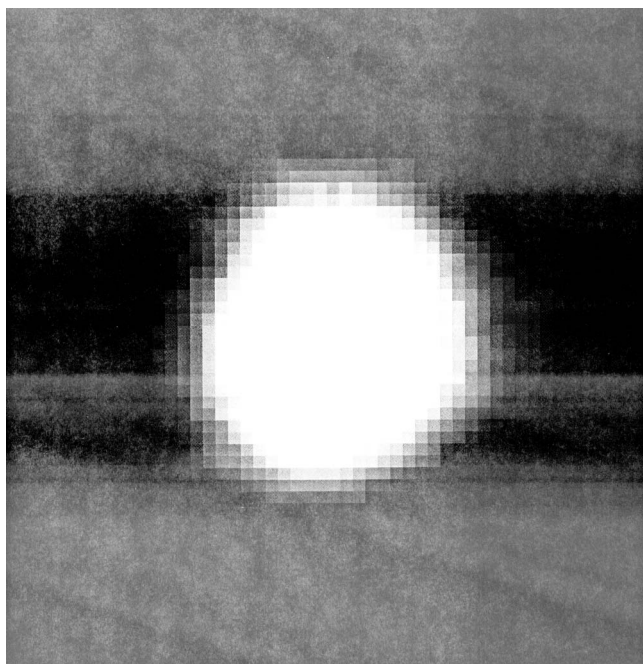


**Fig. 4** End-on image of an arc operated in the steady mode: 800 A, 60 slm Ar, straight gas injection

attachment itself stays in the same location, followed by a breakdown occurring either between the arc column and anode surface or between the arc column and the distorted attachment channel. However, in our experiments, we have not observed the second restrike mode. The arc attachment is moving in the swirl flow direction in the restrike mode and the takeover mode, when the swirl-flow gas injector and the partially swirl-flow gas injector are used. With the straight-flow gas injector, the movement is not easily observed since the movement is predominantly in the direction perpendicular to the imaging plane. However, changing of the focal plane to make an image of the arc attachment visible suggests that a moving arc attachment exists.

The side view of the plasma jet indicates that the fluctuation of the jet appearance is very complex. The jet length keeps changing. The jet body, especially the part near the nozzle exit, keeps expanding and shrinking, while the jet axis oscillates in the radial direction. The centerline of the plasma jet can make snakelike movement, while the tip of the jet fluctuates randomly. The fluctuations of the jet length and width have the same frequency as the arc fluctuations inside the nozzle.

### 3.1 Description of Different Modes

In the steady mode, the arc has a fixed length, and the small ripple on the voltage trace might come from the irregularity of the power supply or the gas flow. Figure 4 shows an end-on image of the arc operated in the steady mode, which is obtained with pure argon, a straight flow, a current of 800 A, and a flow rate of 60 slm; the corresponding arc voltage is 22.4 V. From this image, we can see that the diameter of the arc column is very large. No distinguished arc attachment can be seen. The reason for this phenomenon is that the arc actually attaches to the anode just in the nozzle entrance.

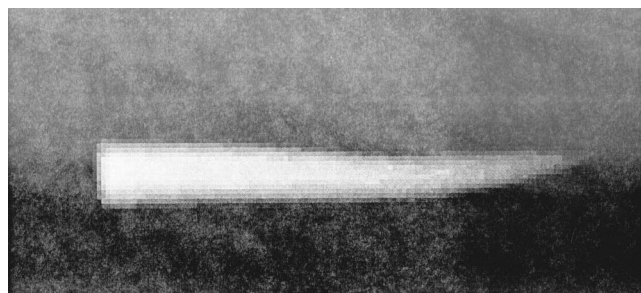


**Fig. 5** Jet image of an arc operated in the steady mode; same conditions as in Fig. 4

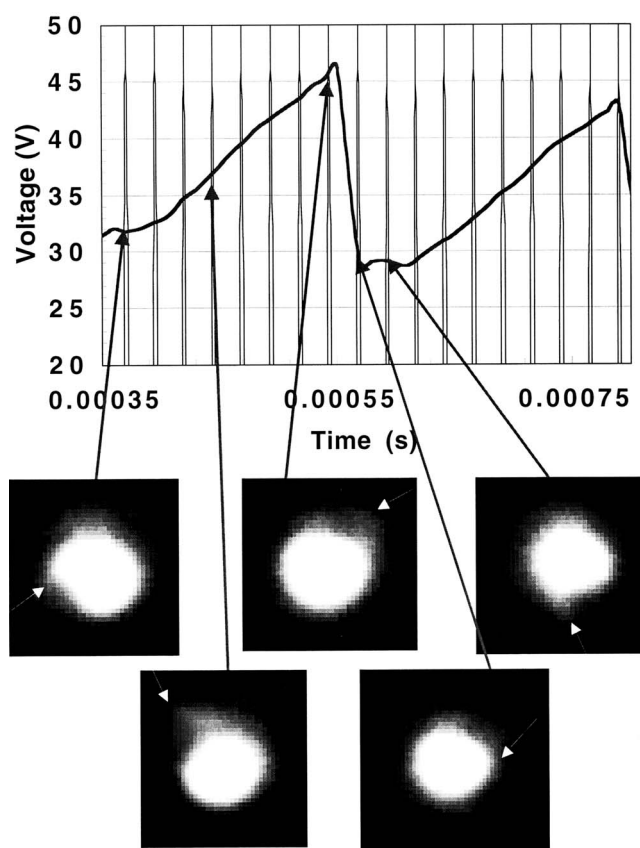


**Fig. 6** Voltage waveform and end-on images of an arc operated in the restrike mode: 200 A, 98/20 slm Ar/He flow, swirl injection

The side view of the jet in the steady mode shows that the jet is long and thin (Fig. 5). Since the arc has a very low voltage and a low torch efficiency, the energy actually transferred to the jet is relatively low. Because of the stable arc, the jet with the steady mode has a laminar-like appearance rather than a turbulent one. This can be confirmed by the low noise of the jet. The low level of turbulence results in the long jet despite the low power level of the arc operation.

Figures 6 and 7 show the voltage traces of the torch operated with the swirl gas flow and the corresponding arc end-on images. In Fig. 6, which is obtained with a current of 200 A and

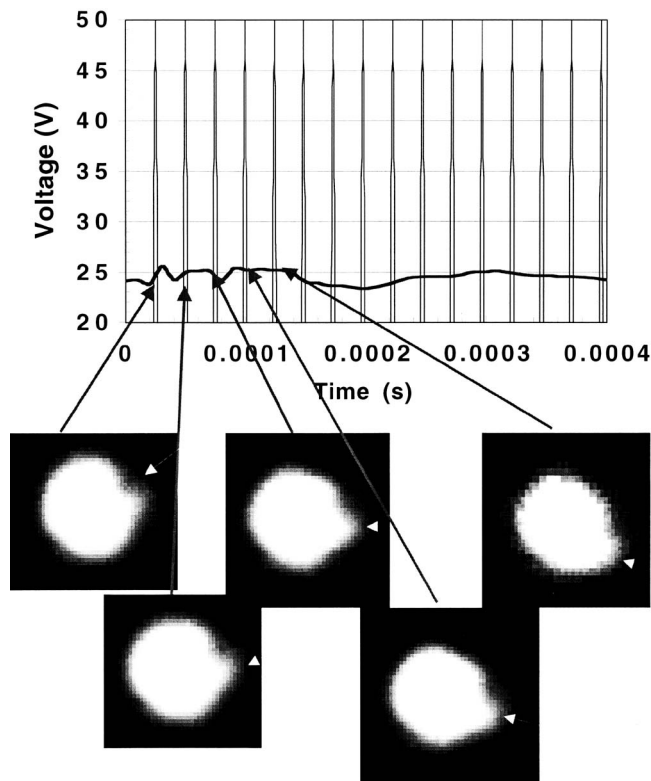


**Fig. 7** Voltage waveform and end-on images of an arc operated in the takeover mode: 800 A, 58/20 slm Ar/He flow, swirl injection

a gas flow of 98/20 slm for argon/helium, the arc is operated in a restrike-dominated mode (mode = 1.8), and a marker is used to indicate the location of the arc attachment. Figure 7 shows the arc operated in a takeover-dominated mode (mode = 0.8), which is obtained with a current of 800 A and a gas flow of 58/20 slm for argon/helium. The arc column with the restrike mode is about 5.6 mm in diameter, and the one with the takeover mode is about 6.3 mm. Consequently, the thickness of the cold-gas boundary layer of the former is larger than that of the latter.

The arc with restrike mode has a clearly defined attachment, and in one cycle of the arc voltage fluctuation, the arc attachment moves three-quarters of the perimeter around the anode surface. This characteristic can be interpreted as an arc attachment starting at a specific location and an upstream breakdown occurring when the arc reaches a certain length. Alternatively, it could be that the arc attachment travels along a preferred path created by wear, or it could be a combination of both.

On the other hand, the arc with takeover mode attaches to the anode surface with a broad root. This root travels only 30 to 60° of the perimeter around the anode surface. The relatively small amplitude of the arc voltage fluctuation indicates a small movement of the arc attachment in axial direction. For this thin cold-gas boundary layer situation, the average temperature and the electric field in the boundary layer are so high that the previous attachment will not vanish instantly when the breakdown occurs, and the arc current gradually transfers to the new attachment. An estimate of the electric field may be obtained from the following considerations. For typical restrike conditions, we

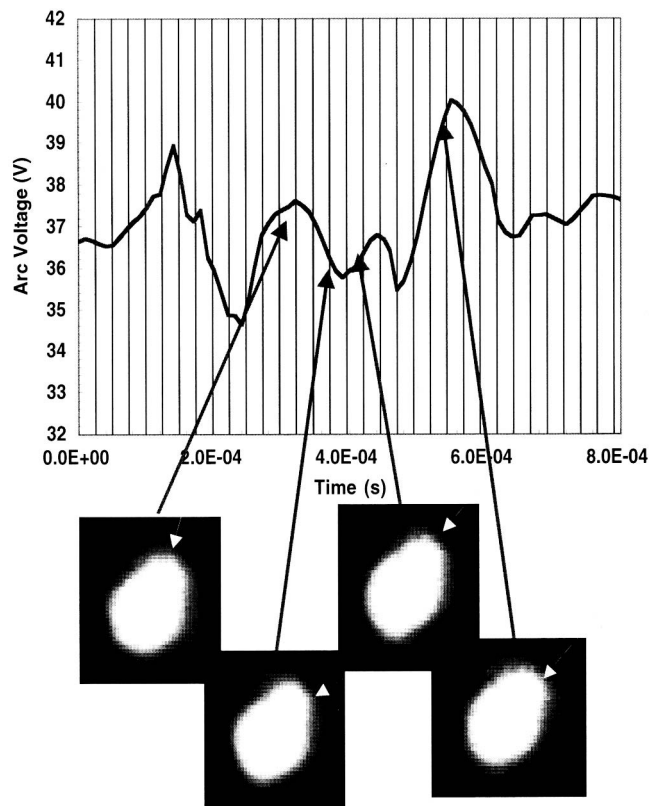


**Fig. 8** Voltage waveform and end-on images of an arc operated with a new anode: 500 A, 58/20 slm Ar/He flow, swirl injection

have a maximum arc voltage of about 90 V and a boundary layer thickness of about 1.2 mm. If we subtract a voltage drop in the cathode region of about 15 V, we have a maximum potential difference of 75 V between the arc and the anode surface. This translates into an average field of 62.5 kV/m across the boundary layer in this region. The effect of gradual transfer of the current from one attachment to the next has been observed previously by using a segmented anode.<sup>[8]</sup> A comparison of the voltage traces obtained with the plasma spray torch and those with the segmented anode lead us to believe that the gradual transfer of the current takes place and is represented by a more symmetrical voltage waveform.

### 3.2 Effects of Different Anodes

The surface condition of the anode can strongly affect the behavior of the arc attachment. Figures 8 and 9 show the end-on images and voltage traces of arcs with different anodes and the same operating parameters: arc current of 500 A, an argon/helium flow rate of 58/20 slm, and a swirl flow. Again, markers are used to indicate the location of the arc attachment. Figure 8 is obtained with the new anode, and Fig. 9 is obtained with the burnt anode. The operating parameters make the arc operate in the takeover-dominated mode with both anodes (mode = 0.8 and mode = 1).

The differences between these two figures are obvious. In Fig. 8, the arc shows a high mean voltage with a low fluctuation. The average thickness of the cold-gas boundary layer, in this

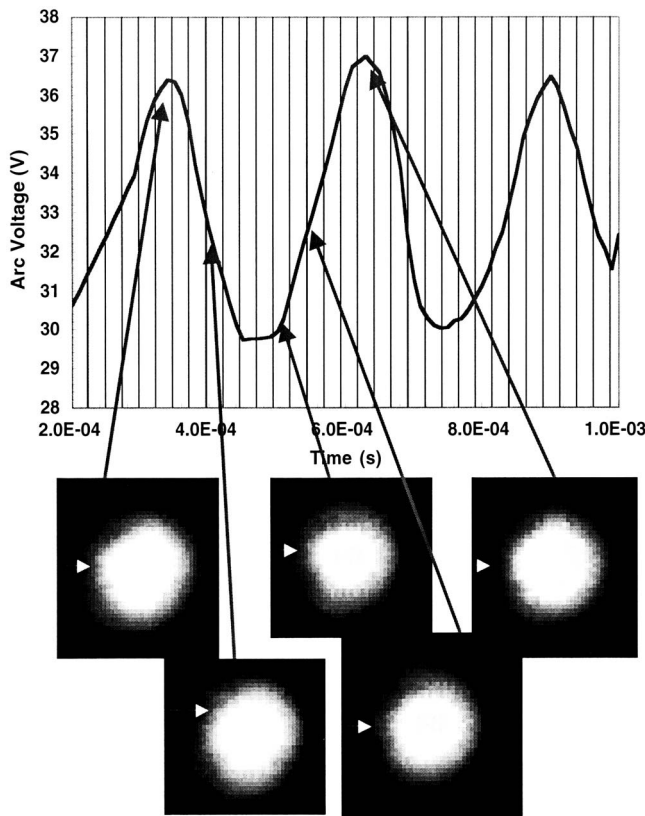


**Fig. 9** Voltage waveform and end-on images of an arc operated with a burnt anode; same conditions as in Fig. 8

case, is about 0.75 mm, while the thickness with the burnt anode is about 0.71 mm. Even though the value for the boundary layer thickness with the burnt anode is reproducibly determined to be smaller, it is within the standard deviation of this measurement. We have to conclude that, in this case, the anode surface condition plays a role in determining the operating mode. The arc attachment moves in a small range around the perimeter of the anode, about  $30^\circ$ . The higher mean voltage indicates that the arc attachment oscillates around a downstream location compared to the attachment with the burnt anode. In the case of a burnt anode, the arc has a relative low voltage with high amplitude fluctuations in Fig. 9. The low mean voltage indicates that the arc is shorter. However, even with a relatively large fluctuation amplitude, the arc attachment shows little movement in the circumferential direction. This means that the arc travels along a certain preferred path on the anode surface, and the swirl flow has less effect on the arc attachment movement in a strongly eroded anode. The thinner boundary layer in the case of the eroded anode may be a result of increased turbulence due to the surface irregularity. The large fluctuating amplitude should be caused by the axial movement of the arc attachment, even a distorted attachment channel with a stationary attachment may take place if the anode surface condition prevents the arc attachment from moving.

The arc operated with the in-used anode, as expected, shows characteristics between the two extreme cases, as described previously.

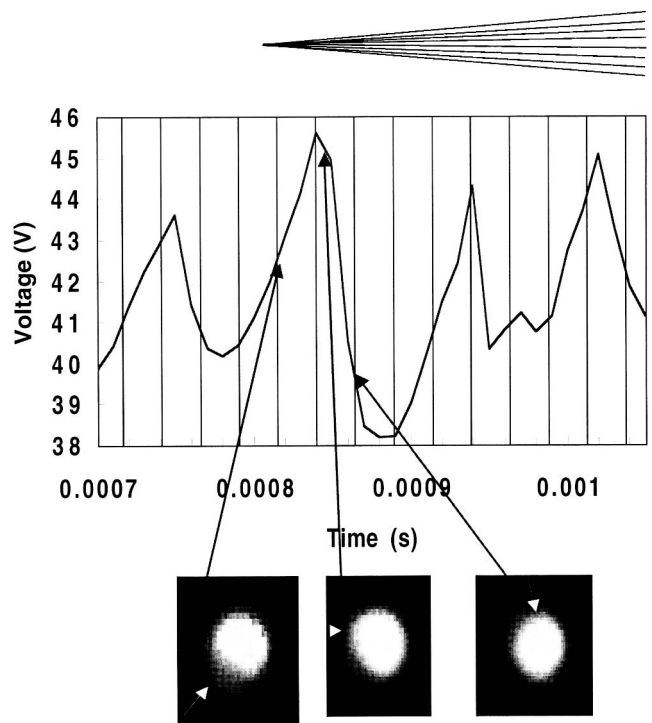


**Fig. 10** Voltage waveform and end-on images of an arc operated with a swirl gas injector: 500 A, 98/40 slm Ar/He flow

### 3.3 Effects of the Gas Injection Methods

We have used different gas injectors to produce different gas-flow configurations in the torch. Figures 10 and 11 show the voltage trace with high-speed images obtained with swirl gas flow and straight flow, respectively. All these voltages and images are obtained with an argon/helium mixture, a current of 500 A, and a flow rate of 98/40 slm. All the voltages show a restrike-takeover mixed mode and a clearly visible arc attachment. The mode values are 1.3 and 1.4, respectively. The arc operating with swirl flow has the higher mean voltage, but the fluctuation amplitudes have similar values for all three cases.

Comparing the images obtained with the different plasma-gas injectors, we can see in Fig. 10 that the arc with swirl flow has a relatively broad attachment, and the attachment moves over half of the perimeter of the anode surface. In Fig. 11, obtained with straight flow, the arc attachments are constricted. Rather than moving around the anode surface, the arc attachments jump from one spot to another. With the partial swirl-gas injector, the arc attachment can be also observed with a small circumferential movement between the jumps. The arc operated with swirl flow has a higher frequency and slightly smaller mode value than the arc with straight flow. This means that the swirl flow can randomize the location of the breakdown and lead the arc toward the takeover mode.

An important observation is that an anode jet is observed with straight gas flow when the arc is operated in the restrike mode. With the straight flow, we can see that the anode jet pushes the arc column off the centerline of the nozzle and distorts the cross section of the arc column, facilitating a breakdown on the opposite side of the arc column. The anode jet is hardly observed with the swirl flow, possibly because the magnetic pressure gradient that generates the jet is not directed in the radial direction but in the direction of the swirl.

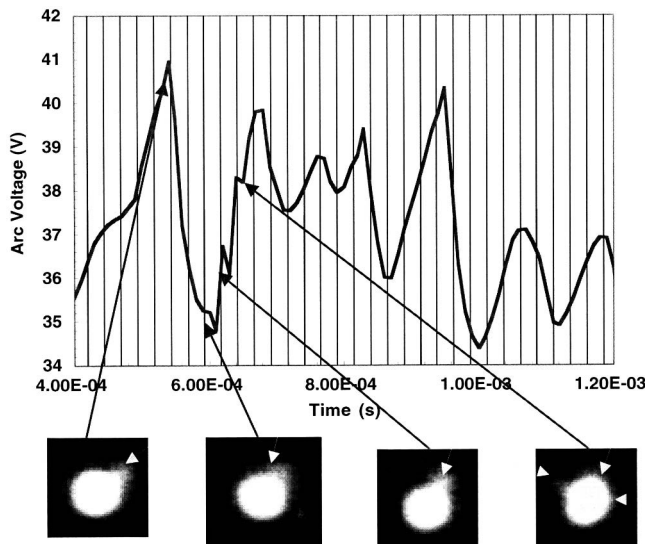


**Fig. 11** Voltage waveform and end-on images of an arc operated with a straight gas injector: 500 A, 98/40 slm Ar/He flow

It is also observed that the arc may have several simultaneous attachments. However, most of the multiple attachments are very short-lived, and one attachment becomes dominant. In particular, we can see that the old anode attachment exists for a while after a new attachment appears. This observation confirms the description of the takeover mode and explains the time delay on the down slope of the voltage waveform.

### 3.4 Quantification of the Arc Modes

The dependence of the arc mode value on the operating parameters is given in Fig. 12. These mode values are obtained with the new anode. In Fig. 12, an argon/helium flow of 58/20 slm is the same mass flow rate as a pure argon 60 slm, and 98/20 slm is the same as 100/00 slm. No pure restrike mode appears with a current above 500 A. With an increasing arc current, a decreasing mass flow rate, and a decreasing helium ratio, the arc mode value decreases. All those changes in operating parameters represent a decrease in the thickness of the cold-gas boundary layer.

The arc mode value has a wide range from 0 to 1.5 with the straight flow and a narrow range from 0.2 to 1.2 with the swirl flow. A rapid transition in the arc operation occurs when the current increases in the upper ranges (above 700 A), in which the arc jumps from a takeover-dominated mode (usually mode value = 0.8 to 1) to a steady-dominated mode (mode value < 0.2). Such a rapid change has not been observed with the swirl flow. This could be explained by the fact that the swirl flow leads to a stronger constriction of the arc column and, thus, has a stronger drag force acting on the anode attachment. It can be seen from Fig. 12 that for both flow configurations a plateau exists in the mode-value contour plots, indicating the existence of a range of operating parameters for which there is only a small change in mode value. The mode values for this plateau are in the range of 0.8 to 1, and the plateau is somewhat larger for the swirl flow condition. According to our observations, operation in the takeover mode (mode value around 1) gives the most consistent coating

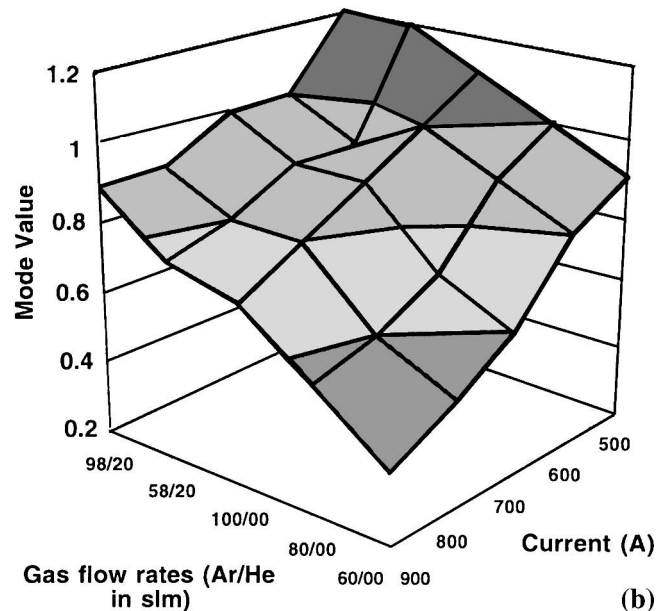
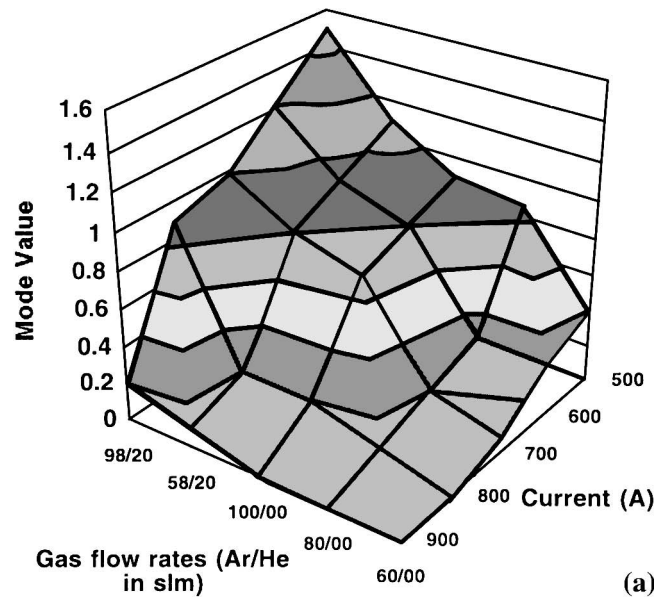


**Fig. 12** Dependence of the arc mode value on the operating parameters with (a) a straight flow and (b) a swirl flow

quality with the SG-100 torch, and the operating parameter values recommended by the manufacturer for a new anode will assure operation in this mode. Figure 12 indicates by how much one can deviate from the recommended setting without changing the operating mode.

## 4. Conclusions

A combination of voltage trace analysis and high-speed video imaging of the arc in a commercial plasma torch has led to the following observations.

- Three distinctive operating modes of the plasma torch exist: the restrike mode, the takeover mode, and the steady mode.



These modes can be quantified through analysis of the voltage trace.

- The operating modes are clearly correlated with the thickness of the cold-gas boundary layer between the arc and the anode nozzle wall. In general, a thicker boundary layer leads to a restrike mode, while a thin boundary layer favors a steady mode.
- Increasing the arc current and decreasing the flow rate will decrease the boundary layer thickness.
- An eroded anode shows a thinner boundary layer and a reduced motion of the arc attachment, but it may also lead to a more strongly distorted arc column. The consequence is the operation closer to a restrike mode.
- A swirl flow may result in a more constricted arc, but the anode attachment movement is randomized favoring the operation in the takeover mode.
- Coating analysis has shown that most consistent results are obtained with random fluctuations with small amplitudes, as offered by the takeover mode operation.
- A contour map of the mode value as function of the principal operating parameters for the SG-100 torch offers a way to estimate the amount by which the recommended operating parameter values can be varied without change of operating mode.

## Acknowledgments

This work has been supported, in part, by the National Science Foundation through grant No. CTS-9903950 and by the Center for Plasma-Aided Manufacturing.

## References

1. Z. Duan, K. Wittmann, J.F. Coudert, J. Heberlein, and P. Fauchais: *Proc. 14th Int. Symp. on Plasma Chemistry*, M. Hrabovsk'y, M. Konrád, and V. Kopeck'y, ed., Institute of Plasma Physics AS CR, Prague, Czech Republic, 1999, pp. 233-38.
2. Z. Duan, J. Heberlein, S. Janisson, K. Wittmann, J.F. Coudert, and P. Fauchais: *Tagungsband Conf. Proc.*, E. Lugscheider and P.A. Kammer, ed., ASM International, Materials Park, OH, 1999, pp. 247-52.
3. M.P. Planche, Z. Duan, O. Lagnoux, J. Heberlein, J.F. Coudert, and P. Fauchais: *Proc. 13th Int. Symp. Plasma Chemistry*, C.K. Wu, ed., Peking University Press, Beijing, 1997, pp. 1460-65.
4. S. Wutzke, E. Pfender, and E. Eckert: *AIAA*, 1967, 5(4), pp. 1216-32.
5. M.I. Boulos, P. Fauchais, and E. Pfender: *Thermal Plasmas: Fundamentals and Applications*, Plenum Publishing, New York, NY, 1994, 1.
6. J.F. Coudert, M.P. Planche, and P. Fauchais: *Plasma Chem. Plasma Processing*, 1995, 16(1), pp. 211s-27s.
7. J.F. Coudert, M.P. Planche, and P. Fauchais: *Plasma Chem. Plasma Processing*, 1995, 15(1), pp. 47-70.
8. D.H. Berns: Master's Thesis, University of Minnesota, Minneapolis, MN, 1994.